Hydrodynamic trap for single particles and cells

Melikhan Tanyeri,[1] Eric M. Johnson-Chavarria,[2] and Charles M. Schroeder[1,2,a)]
[1]*Department of Chemical and Biomolecular Engineering, University of Illinois at Urbana-Champaign, Urbana, Illinois 61801, USA*
[2]*Center for Biophysics and Computational Biology, University of Illinois at Urbana-Champaign, Urbana, Illinois 61801, USA*

(Received 31 March 2010; accepted 24 April 2010; published online 2 June 2010)

Trapping and manipulation of microscale and nanoscale particles is demonstrated using the sole action of hydrodynamic forces. We developed an automated particle trap based on a stagnation point flow generated in a microfluidic device. The *hydrodynamic trap* enables confinement and manipulation of single particles in low viscosity (1–10 cP) aqueous solution. Using this method, we trapped microscale and nanoscale particles (100 nm–15 μm) for long time scales (minutes to hours). We demonstrate particle confinement to within 1 μm of the trap center, corresponding to a trap stiffness of $\sim 10^{-5}$–10^{-4} pN/nm. © *2010 American Institute of Physics*.
[doi:10.1063/1.3431664]

The ability to trap particles, molecules, and atoms has revolutionized many fields of science and engineering. Over the past two decades, a diverse set of methods based on optical,[1] electrokinetic,[2,3] magnetic,[4,5] acoustic,[6] and hydrodynamic forces[7–12] has been developed to confine and manipulate microscale and nanoscale particles in aqueous solution through direct control of particle position and velocity. Overall, these methods have been used to investigate a wide-array of physical and biological problems, and each method exhibits a clear set of advantages and limitations as tools for studying living cells and biological systems.

Hydrodynamic forces have been used in both contact-based[12] and noncontact[7–11] methods to confine and manipulate particles. Contact-based methods are efficient in trapping very large numbers of particles to form dynamic arrays for high-throughput studies, albeit with limited ability for fine-scale manipulation of single particles. Noncontact methods currently rely on either stagnation point flows[7–10] or microeddies.[11] Particle confinement based on stagnation point flows can provide high resolution manipulation of single particles. However, previous work has mainly focused on trapping macroscopic (millimeter-sized) particles in aqueous solutions[7] or confinement of microscopic (micron-sized) particles in highly viscous solutions.[10] In addition, passive stagnation point flows have been used to observe the dynamics of single DNA polymer chains for extended time scales.[8,9]

In this paper, we report an automated particle trapping and manipulation method, the *hydrodynamic trap*, which offers high resolution confinement of single microscale and nanoscale particles in low viscosity (1–10 cP) aqueous solution by using a stagnation point flow generated in a microfluidic device. The underlying principle of the hydrodynamic trap is active feedback control of a stagnation point flow field in order to guide particles to the trap center (setpoint position) and maintain the center-of-mass position of the trapped particle at the trap center in two dimensions. In this work, we demonstrate trapping of submicron sized particles (100 nm) and confinement of micron-sized particles with high resolution (to within 1 μm) for extended time scales (>10 minutes).

The hydrodynamic trap consists of a hybrid polydimethylsiloxane (PDMS)/glass microfluidic device[13] with a cross-slot channel geometry [Fig. 1(a)]. Two laminar inlet streams converge at the channel junction from opposing directions and form two divergent outlet streams, which exit the junction through the perpendicular channels in opposite directions. The cross-slot microchannel geometry creates a planar extensional flow which contains a stagnation point, or point of zero velocity, at the center of channel junction [Fig. 1(b)]. A planar extensional flow is described by a two-dimensional flow field consisting purely of extensional and compressional components with no rotational character. The axes along the inlet and outlet streams are called the compressional (x) and extensional (y) axes, respectively. Local analysis can be applied to the flow field in the vicinity of the microchannel junction such that the velocity field (v_x, v_y) is given by[14]

$$\vec{\mathbf{v}} = \dot{\varepsilon}(-x, y), \tag{1}$$

where $\dot{\varepsilon}$ is the fluid strain rate and (x, y) is the particle position with respect to the stagnation point. In addition, a planar extensional flow can be described by a velocity potential function φ [Fig. 1(b)] representing a semistable potential

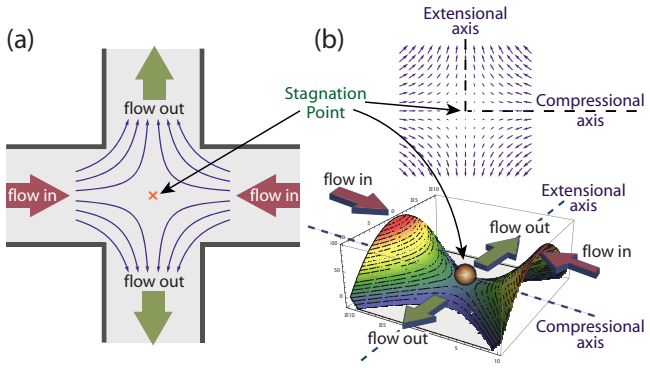

FIG. 1. (Color online) (a) A hydrodynamic trap is created by a planar extensional flow field at the junction of two perpendicular microchannels. (b) The velocity field (top) and the potential well (bottom) for a particle in the flow field at the microchannel junction.

a)Author to whom correspondence should be addressed. Electronic mail: cms@illinois.edu.

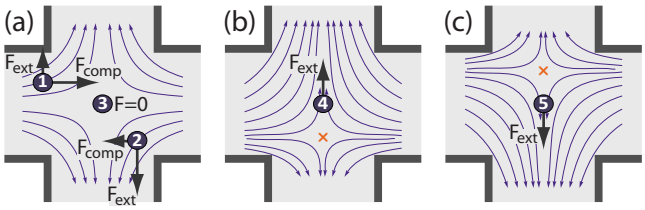

FIG. 2. (Color online) (a) Hydrodynamic forces acting on particles in the flow field. (b) and (c) Steering the particle by manipulating the stagnation point (cross) along the extensional axis.

well (saddle surface) and a stagnation point (saddle point)[14]

$$\varphi = (\dot{\varepsilon}/2)(y^2 - x^2). \quad (2)$$

Along the compressional axis, the stagnation point is a stable equilibrium point (local minimum in the potential energy of the trap); however, the stagnation point represents an unstable equilibrium point (local maximum) along the extensional axis.

A particle entering the microchannel junction is subject to a net hydrodynamic force proportional to the local magnitude of the flow field [Fig. 2(a), see particles 1 and 2]. Along the compressional axis, the particle experiences an *attractive* force toward the stagnation point; on the contrary, a *repulsive* force (pointing away from the stagnation point) is exerted on the particle along the extensional axis. As a result, a *passive* trap is achieved along the compressional axis, and *active* flow control is required to confine a particle along the extensional axis. In an ideal trap, a particle positioned exactly at the stagnation point experiences zero net force and velocity [Fig. 2(a), particle 3] and therefore remains trapped at the stagnation point unless it is perturbed by a Brownian fluctuation.

In the hydrodynamic trap, we implement active flow control along the extensional axis to maintain particle center-of-mass position at the trap center, which is analogous to balancing an inverted pendulum. In the absence of active flow control, particles may exhibit long residence times at or near the stagnation point but ultimately escape due to Brownian fluctuations coupled with fluid convection along the extensional axis. In the trap, fluid flow is controlled to precisely position the stagnation point with respect to particle position along the extensional axis. Specifically, we use an integrated microfluidic device with an on-chip metering valve located in one of the outlet channels. This valve is used to regulate the relative flow rates in the outlet streams, which enables micron-scale control over the stagnation point position.[15] Using this method, it is possible to exert zero net force [Fig. 2(a), particle 3], or exert forces in opposite directions with variable magnitude [Figs. 2(b) and 2(c), particles 4 and 5] for any particle at the microchannel junction by simply manipulating the flow field along the extensional axis. The magnitude of the force is proportional to the distance between the particle and the stagnation point, and the small scale changes induced in the flow do not measurably affect fluid strain rates or flow character.[9]

As an initial demonstration of the hydrodynamic trap, we fabricated a two-layer PDMS/glass hybrid microfluidic device using multilayer soft-lithography techniques.[15–17] The microfluidic device consists of a fluidic layer positioned between a glass substrate and a control layer. The fluidic layer contains a cross-slot channel geometry to generate a planar extensional flow. A thin elastomeric membrane

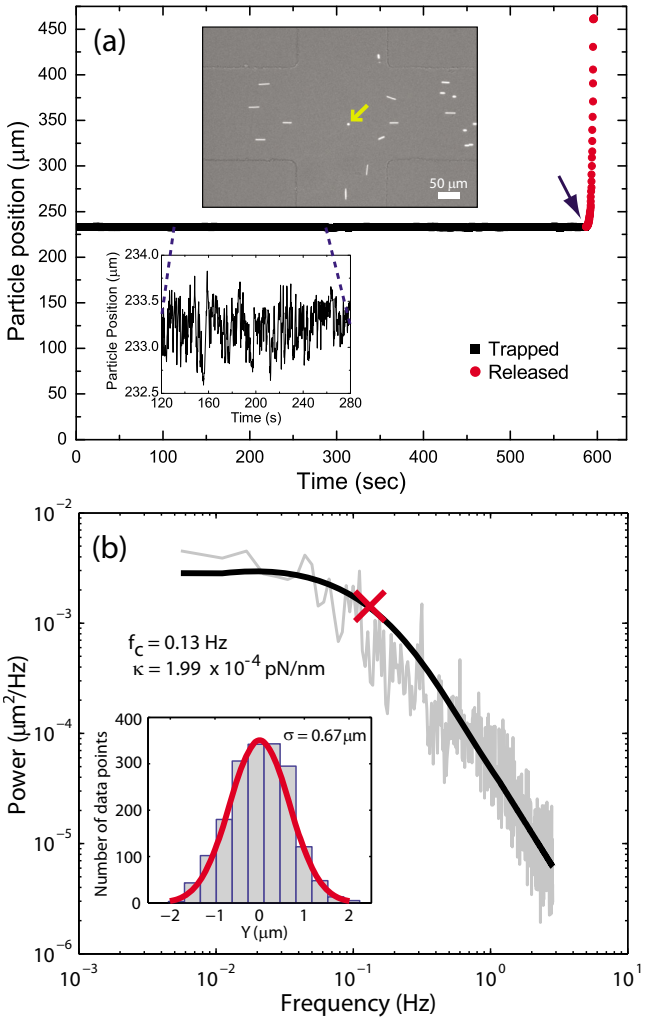

FIG. 3. (Color online) (a) Trajectory for a trapped particle along the extensional axis (squares). When the particle is released from the trap (arrow), it escapes along one of the outlet channels (circles). Insets: (Bottom) Rescaled particle trajectory between 120–280 s. (Top) Micrograph of a bead trapped at the stagnation point. (b) Power spectrum of a trapped polystyrene bead (2.2 μm diameter) along the extensional axis. Inset: Histogram of displacements of a trapped bead (2.2 μm diameter) from the trap center.

(30–100 μm) separates the fluidic and control layers and may be deflected downwards onto the fluidic layer by applying pressure to the control layer.[16] Through membrane deflection, the cross-sectional area of the fluidic channel beneath the control layer is changed to adjust flow resistance. In this manner, the control layer acts as a dynamic pneumatic valve controlling flow rates in the fluidic layer, thereby enabling fine-scale control of stagnation point position and particle confinement. A feedback control algorithm is used for particle tracking and confinement.[15]

To demonstrate proof-of-principle of the hydrodynamic trap, we trapped fluorescent and nonfluorescent polystyrene beads of various size (fluorescent: 100, 540, 830 nm, and 2.2 μm; nonfluorescent: 1.23, 2.2, 5, 9, and 15 μm diameter).[15] The trajectory of a trapped fluorescent bead (2.2 μm diameter) along the extensional axis is shown in Fig. 3(a). The bead is initially trapped (squares) for nearly 10 min and is then released from the trap and escapes along one of the outlet channels (circles). The trapped particle is confined to within ± 1 μm for several minutes using a proportional controller ($K_p = -1.75$).

In addition to particles, we also trapped single live *Escherichia coli* bacterial cells in Luria–Bertani (LB) broth medium. Trapped cells were imaged using phase contrast microscopy, which provided images with adequate resolution to enable confinement by the feedback controller. Single cells were trapped for several minutes in free solution and exhibited active and directed transport, characteristic of bacterial "swimming" motion.

We characterized the trap stiffness by measuring the power spectral density of position fluctuations for a trapped particle. Fluctuations in particle position arise due to convection (active flow control) and thermal fluctuations (Brownian motion). The particle is bound by a harmonic potential along the compressional axis, where trap stiffness scales linearly with the strain rate. Along the extensional axis, the particle experiences a pseudopotential well created by the active manipulation of the stagnation point by the feedback controller. Trap stiffness along this axis depends on the strain rate, particle size, viscosity, and feedback loop response time.

As expected, the measured power spectrum for particle position fluctuations along the compressional axis is well-described by a Lorentzian[15] from which we extract the trap stiffness, $k=1.24\times10^{-4}$ pN/nm. Along the extensional axis, for small values of proportional gain, the particle position is stable and the power spectrum is represented by a Lorentzian.[4] Figure 3(b) shows the measured power spectrum for particle position fluctuations along the extensional axis with the corresponding Lorentzian fit ($k=1.99\times10^{-4}$ pN/nm). At large values of the proportional gain, *ringing* occurs and the trapped particle oscillates, which appears as a peak in the power spectrum in the vicinity of the corner frequency (data not shown). To complement experimental results, we performed Brownian dynamics simulations for a particle confined in the hydrodynamic trap, and the results are in good agreement with the experimental power spectra.[15] In general, hydrodynamic trap stiffness values are comparable to those achieved with magnetic and electrophoretic traps.[3,4]

Hydrodynamic trap stiffness is given by a balance between thermal energy E^{thermal} and trap energy E^{trap}. Along the compressional axis, particles are passively trapped by fluid flow, and the hydrodynamic force F^{Hyd} exerted on a particle is given by $F^{\text{Hyd}}=kx$, where k is the trap stiffness. Assuming laminar flow conditions and a point particle, trap stiffness may be expressed as $k=6\pi\eta R\dot{\varepsilon}$. In initial experiments, we trapped a 2.2 μm diameter bead in 11 cP solution in fluid strain rate of 1 s^{-1}, yielding a trap stiffness of $\sim2\times10^{-4}$ pN/nm, which is in good agreement with the measured compressional axis trap stiffness.[15]

The hydrodynamic trap enables confinement of particles with nanoscale to microscale dimensions in aqueous solution and offers several advantages as a trapping method. First, hydrodynamic trapping is feasible for any particle with no specific requirements on the material composition or the chemical/physical nature of the trapped object. Second, due to the semi-stable nature of the trapping potential, the hydrodynamic trap inherently enables confinement of a single "target" object in dilute or concentrated particle or cell suspensions, which is a key advantage for a trapping method. Indeed, the ability to trap a single particle in a crowded solution represents a key advantage for a trapping method. Third, the hydrodynamic trapping force for point particles scales linearly with particle radius, whereas trapping forces for optical, paramagnetic, diamagnetic, acoustic, and dielectrophoretic traps all scale with particle volume. Therefore, the hydrodynamic trap is expected to enable straightforward confinement and manipulation of small nanoparticles (<100 nm) in solution. Fourth, the hydrodynamic trap functions as a simple integrated microfluidic device without the need for complex device synthesis, patterned electrodes, or coupling optical or magnetic fields into the device. Finally, we anticipate that the hydrodynamic trap will provide an ideal platform to confine and study living cells in free-solution for long times (hours) in a nonperturbative fashion, as this method of trapping does not rely on application of optical or electric fields. In summary, the hydrodynamic trap provides a viable alternative platform for observation of biological and nanomaterials without surface immobilization while allowing for varying the surrounding medium conditions in real-time.

This work was funded by an NIH Pathway to Independence (PI) Award, under Grant No. 4R00HG004183-03.

[1] A. Ashkin, J. M. Dziedzic, J. E. Bjorkholm, and S. Chu, Opt. Lett. **11**, 288 (1986); K. C. Neuman and S. M. Block, Rev. Sci. Instrum. **75**, 2787 (2004); D. G. Grier, Nature (London) **424**, 810 (2003); A. H. J. Yang, S. D. Moore, B. S. Schmidt, M. Klug, M. Lipson, and D. Erickson, *ibid.* **457**, 71 (2009).
[2] P. Y. Chiou, A. T. Ohta, and M. C. Wu, Nature (London) **436**, 370 (2005); A. E. Cohen and W. E. Moerner, Appl. Phys. Lett. **86**, 093109 (2005); A. Ramos, H. Morgan, N. G. Green, and A. Castellanos, J. Phys. D **31**, 2338 (1998); M. D. Armani, S. V. Chaudhary, R. Probst, and B. Shapiro, J. Microelectromech. Syst. **15**, 945 (2006).
[3] A. E. Cohen, Phys. Rev. Lett. **94**, 118102 (2005).
[4] C. Gosse and V. Croquette, Biophys. J. **82**, 3314 (2002).
[5] H. Lee, A. M. Purdon, and R. M. Westervelt, Appl. Phys. Lett. **85**, 1063 (2004).
[6] H. M. Hertz, J. Appl. Phys. **78**, 4845 (1995); M. Evander, L. Johansson, T. Lilliehorn, J. Piskur, M. Lindvall, S. Johansson, M. Almqvist, T. Laurell, and J. Nilsson, Anal. Chem. **79**, 2984 (2007).
[7] G. I. Taylor, Proc. R. Soc. London **146**, 501 (1934); B. J. Bentley and L. G. Leal, J. Fluid Mech. **167**, 219 (1986).
[8] T. T. Perkins, D. E. Smith, and S. Chu, Science **276**, 2016 (1997).
[9] C. M. Schroeder, H. P. Babcock, E. S. G. Shaqfeh, and S. Chu, Science **301**, 1515 (2003).
[10] P. R. Start, S. D. Hudson, E. K. Hobble, and K. B. Migler, J. Colloid Interface Sci. **297**, 631 (2006).
[11] B. R. Lutz, J. Chen, and D. T. Schwartz, Anal. Chem. **78**, 5429 (2006); C. M. Lin, Y. S. Lai, H. P. Liu, C. Y. Chen, and A. M. Wo, *ibid.* **80**, 8937 (2008).
[12] D. Di Carlo, L. Y. Wu, and L. P. Lee, Lab Chip **6**, 1445 (2006); W. H. Tan and S. Takeuchi, Proc. Natl. Acad. Sci. U.S.A. **104**, 1146 (2007); A. M. Skelley, O. Kirak, H. Suh, R. Jaenisch, and J. Voldman, Nat. Methods **6**, 147 (2009).
[13] J. C. McDonald and G. M. Whitesides, Acc. Chem. Res. **35**, 491 (2002); S. R. Quake and A. Scherer, Science **290**, 1536 (2000).
[14] G. K. Batchelor, *An Introduction to Fluid Dynamics* (Cambridge University Press, Cambridge, 1967), p. xviii.
[15] See supplementary material at http://dx.doi.org/10.1063/1.3431664 for movies of particle trapping, schematic of the microfluidic device, and power spectra of trapped particle motion along compressional axis.
[16] M. A. Unger, H. P. Chou, T. Thorsen, A. Scherer, and S. R. Quake, Science **288**, 113 (2000).
[17] S. K. Sia and G. M. Whitesides, Electrophoresis **24**, 3563 (2003); T. Thorsen, S. J. Maerkl, and S. R. Quake, Science **298**, 580 (2002); G. M. Whitesides, E. Ostuni, S. Takayama, X. Y. Jiang, and D. E. Ingber, Annu. Rev. Biomed. Eng. **3**, 335 (2001).